Toward a Quasi-dynamic Pulsed Field Electroporation Numerical Model for Cardiac Ablation: Predicting Tissue Conductance Changes and Ablation Lesion Patterns

Richard Simon[1], Nishaki K Mehta[2], Kuldeep B Shah[2], David E Haines[2] and Cristian A Linte[*1,3]

[1]Biomedical Engineering, Rochester Institute of Technology, Rochester, NY, USA
[2]Division of Cardiology, Beaumont Medical Center, Royal Oak, MI, USA
[3]Center for Imaging Science, Rochester Institute of Technology, Rochester, NY, USA

Abstract

Pulsed field ablation (PFA) has the potential to evolve into an efficient alternative to traditional RF ablation for atrial fibrillation treatment. However, achieving irreversible tissue electroporation is critical to suppressing arrhythmic pathways, raising the need for accurate lesion characterization. To understand the physics behind the tissue response PFA, we propose a quasi-dynamic model that quantifies tissue conductance at end-electroporation and identifies regions that have undergone fully irreversible electroporation (IRE). The model uses several parameters and numerically solves the electrical field diffusion into the tissue by iteratively updating the tissue conductance until equilibrium at end-electroporation. The model yields a steady-state tissue conductance map used to identify the irreversible lesion. We conducted numerical experiments mimicking a lasso catheter featuring nine 3-mm electrodes spaced circumferentially at 3.75 mm and fired sequentially using a 1500 V and 3000 V pulse amplitude. The IRE lesion region has a surface area and volume of 780 mm^2 and 1411 mm^3, respectively, at 1500 V, and 1178 mm^2 and 2760 mm^3, respectively, at 3000 V. Lesion discontinuity was observed at 5.0 mm depth with 1500 V, and 7.2 mm depth with 3000 V. This quasi-dynamic model yields tissue conductance maps, predicts irreversible lesion and lesion penumbra at end-electroporation, and confirms larger lesions with higher pulse amplitudes.

1. Introduction

Catheter ablation for the treatment of cardiac arrhythmias, with a specific emphasis on atrial fibrillation (AF), is typically performed using radiofrequency (RF) [1, 2] or cryothermal energy delivery methods, which interrupt the arrhythmic conduction pathway by either heating or freezing the tissue substrate, respectively [3]. Besides RF and cryo ablation, other techniques have been explored and evaluated as potential approaches for tissue ablation, including high-intensity focused ultrasound, microwave, and laser ablation [4]. Nevertheless, the control of ablation can be challenging, leading to incomplete tissue destruction (i.e., reversible tissue ablation) in some cases or excessive destruction that leads to collateral injury to surrounding structures, such as the esophagus, in other cases [5].

Pulsed field ablation (PFA), on the other hand, has the potential to become a promising, new ablation modality for the treatment of cardiac arrhythimas. PFA consists of the delivery of a sequence of high-amplitude electrical pulses of microsecond duration that ablate myocardial tissue by electroporation, with no measurable tissue heating. As such, PFA is a nonthermal ablation technology that ablates tissue through through irreversible electroporation (IRE) — inducing targeted cell death by increasing cell membrane permeability through the application of a high electric field. Given its non-thermal nature and the unique injury characteristics of specific tissue, PFA has the potential to yield superior performance vis-à-vis other traditional thermal-based tissue ablation techniques.

The electric field strength in the SI unit system is expressed in newtons per coulomb (N/C) or volts per meter (V/m), however the typical electric field strength in tissue electroporation dosimetry applications is measured in volts per cm (V/cm). Depending on the strength of the electric field experienced by the cells, the electroporation may result in no effect, reversible electroporation, if the pores in the cell membrane reverse after application of the electric field and the cell survives, or irreversible pore formation, if the pores created in the cell membrane do not reverse after the application of the electric field, leading to cell death.

High voltage electric fields can induce irreversible electroporation with no thermal effects, thanks to the short (i.e., microsecond) duration of the electric field pulses, which allows the dissipation of any resistive heating to conduction and convection. Nevertheless, there exists significant heterogeneity in regard to the strength of the elec-

tric field needed to achieve irreversible electroporation [6–8], typically ranging from 500 to 3000 V/cm.

Although PFA is proposed as a useful modality for cardiac arrhythmia and, specifically AF treatment, several factors determining the electric field distribution, as well as lesion geometry have not been fully characterized. As such, to better understand the physics behind the tissue response to PFA, we propose a quasi-dynamic PFA model that can predict tissue conductance when electroporation equilibrium is achieved, as well as identify tissue regions that undergo irreversible electroporation, enabling the generation of lesion maps that can be used to study lesion depth, including the critical depth at which lesion discontinuities occur.

2. Methods

To study the change of electrical properties of tissue, assumed homogeneous, in response to its exposure to a prescribed electric field distribution, as is the case during electroporation, we developed a quasi-dynamic numerical model that uses several prescribed tissue and electric field parameters to estimate tissue conductance changes, and, in turn, estimate lesion geometry.

The electric field distribution in the synthetic tissue model exposed to an electroporation pulse of voltage u can be determined by solving the equation below for the scalar electrical potential. Moreover, if we neglect transient effects and consider a quasi-dynamic model that only captures the equilibrium state at end-electroporation, we may assume the current density in tissue is divergence-free and the electrical potential satisfies:

$$\nabla \cdot (\sigma \cdot \nabla(u)) = 0, \tag{1}$$

where σ and u represent issue conductance [S/m] and electrical potential [V], respectively.

The applied voltage (model input) was modeled as Dirichlets boundary condition on the contact surface between electrode and tissue geometry. For the model input values, we used the amplitudes of typical electroporation pulses, specifically 1500V or 3000V.

As long as the applied voltage u [V] is sufficiently low, the tissue conductivity [S/cm] can be treated as a constant, and the problem is therefore described by Laplaces equation, which is a linear partial differential equation that can be easily solved numerically. Under constant tissue conductance conditions, the tissue can be modeled as a linear conductor, using linear currentvoltage relationships, since the amplitude of the applied electroporation pulse is too low to produce an electric field E [V/cm] above the reversible electroporation threshold ($E < E_{th}$).

However, according to experimental observations [9], tissue conductance during electrporation is not constant, and hence Eq. (1) becomes nonlinear. Namely, if the local electric field E [V/cm] in the tissue exceeds the E_{th} threshold for reversible electroporation, the electrical properties of the tissue change. Hence, tissue conductance changes with the electric field intensity E (Eq. (2)); specifically, during electroporation, tissue conductance increases (and hence measured impedance decreases) according to its local dependency on the local electric field distribution (E), which, for our model, governs the dynamics of the electroporation process:

$$\sigma = \sigma_0 + \frac{\sigma_1 - \sigma_0}{2}(1 + tanh(k(||E|| - E_{th}))), \tag{2}$$

where $E = -\nabla u$ is the electric field [V/cm], σ is tissue conductance [S/cm], σ_0 is the conductance of non-electroporated tissue, σ_1 is the conductance of fully electroporated tissue, E_{th} is the electric field threshold for reversible electroporation, and k is a fitting parameter that defines the slope of the $\sigma - E$ curve (**Figure 1**).

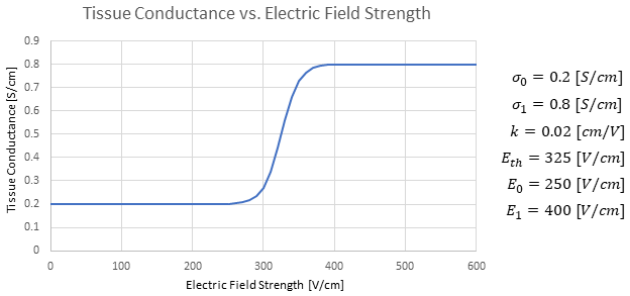

Figure 1. Tissue conductance σ change with electric field strength E, along with the parameters governing the quasi-dynamic electroporation model: σ_0 is the conductance of non-electroporated tissue, σ_1 is the conductance of fully electroporated tissue, E_{th} is the electric field threshold for reversible electroporation, and k is a fitting parameter that defines the slope of the $\sigma - E$ curve.

Our numerical experiments are based on a lasso catheter geometry inspired by the Medtronic Pulmonary Vein Ablation Catheter GOLD (PVAC GOLD) — a 3D, anatomically designed, multiple electrode-catheter used to map, pace and ablate the pulmonary veins (**Figure 2**). The catheter consists of nine 3-mm electrodes distributed along the circumference of a circular lasso catheter, with each electrode spaced at 3.75 mm from its adjacent neighbors. However, as a first order approximation for this initial study, our numerical experiments only consider the 2D circular geometry of the catheter and assume planar contact between the electrodes and tissue surface. Hence, as shown later in our results section, this 2D assumption allows us to "cut and unfold" the circular lesion pattern into a linear pattern and characterize tissue response at various depth along the length of the electroporation pattern.

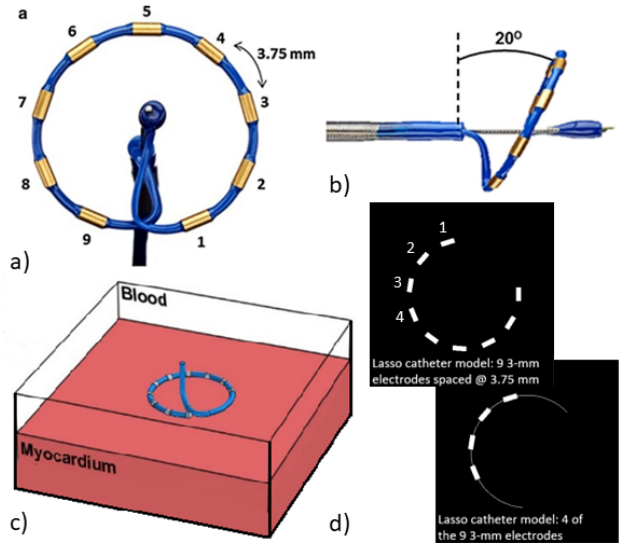

Figure 2. a & b) Images of the Medtronic Pulmonary Vein Ablation Catheter GOLD (PVAC GOLD) lasso catheter based on which we modeled our catheter geometry for this synthetic study; c) schematic representation of the lasso-catheter tissue interaction; and d) image-based representation of the lasso catheter and electrode distribution.

3. Results

We implemented the model using the following parameters: baseline tissue conductance (0.2 S/cm) and electric field strength (200 V/cm), irreversibly electroporated tissue conductance (0.8 S/cm) and electric field strength (450 V/cm), and critical electric field strength for reversible electroporation (200 V/cm). We conducted numerical experiments mimicking the lasso catheter geometry shown in **Figure 2** featuring nine 3 mm electrodes spaced circumferentially at 3.75 mm and fired sequentially at a 1500 V or 3000 V pulse amplitude. The model numerically solves the electric field diffusion into the tissue by iteratively updating the tissue conductance until equilibrium at end-electroporation. The model yields the steady-state tissue conductance map used to identify irreversible lesion and lesion penumbra.

Table 1 summarizes the model-predicted IRE lesion parameters at 1500 V and 3000 V pulse amplitudes.

Table 1. Summary of model-predicted lesion parameters (surface area (mm^2), volume (mm^3), and maximum depth (mm) at 1500V and 3000V pulse amplitude.

Pulse Amplitude / IRE Lesion	1500 V	3000 V
Max IRE Lesion Depth (mm)	5.0	7.2
IRE Lesion Surf Area (mm^2)	780	1178
IRE Lesion Volume (mm^3)	1411	2760

For a pulse amplitude of 1500V (**Figure 3**), the model yielded an irreversible lesion region with a surface area of 780 mm^2 and a volume of 1411 mm^3. Lesion discontinuities were observed at 5.0 mm below tissue surface.

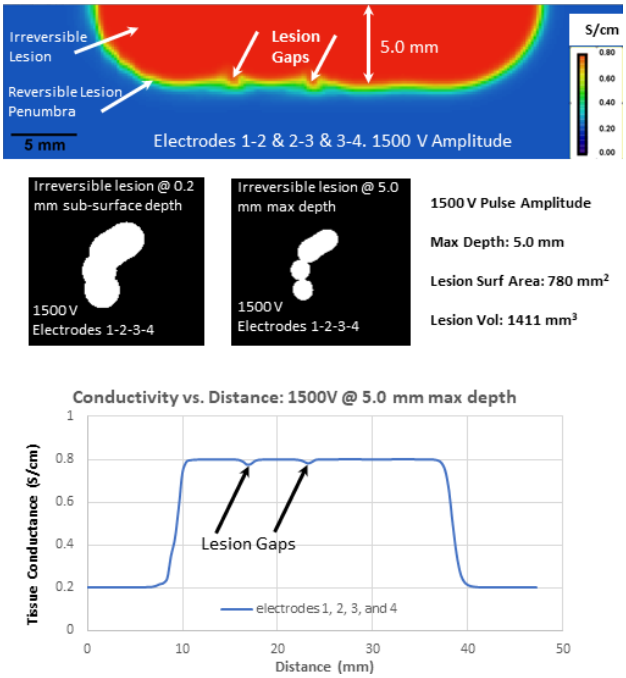

Figure 3. Model-predicted tissue conductance profile and lesion geometry (sub-surface and at max depth) achieved at 1500 V pulse amplitude. Note the onset of gaps at the max connected lesion depth of 5.0 mm.

Similarly, **Figure 4** shows that for a 3000V voltage pulse amplitude, the model yielded an irreversible lesion region with a surface area of 1178 mm^2 and a volume 2760 mm^3. Lesion discontinuities were observed at 7.2 mm below the tissue surface.

Lastly, transverse views through the tissue conductance profiles through the model-predicted lesions (**Figure 5**) at 1500 V and 3000 V pulse amplitude show the difference in the overall geometry of the lesions achieved by sequentially firing electrodes 1 & 2, 1, 2 & 3, and 1, 2, 3 & 4. The tissue conductivity profiles through the model-predicted lesions show the formation of gaps in the IRE lesion pattern at the maximum connected depth of 5.0 mm for the 1500 V pulse amplitude electroporation and 7.2 mm for the 3000 V pulse amplitude electroporation.

Our numerical experiments are in agreement with other studies [9] that suggested tissue conductance is a function of electric field (i.e. σ)and increases during electroporation. Moreover, some preliminary patient and animal studies also reported a decrease in impedance measurements (which inherently implies an increase in tissue conductance) following the application of electroporation

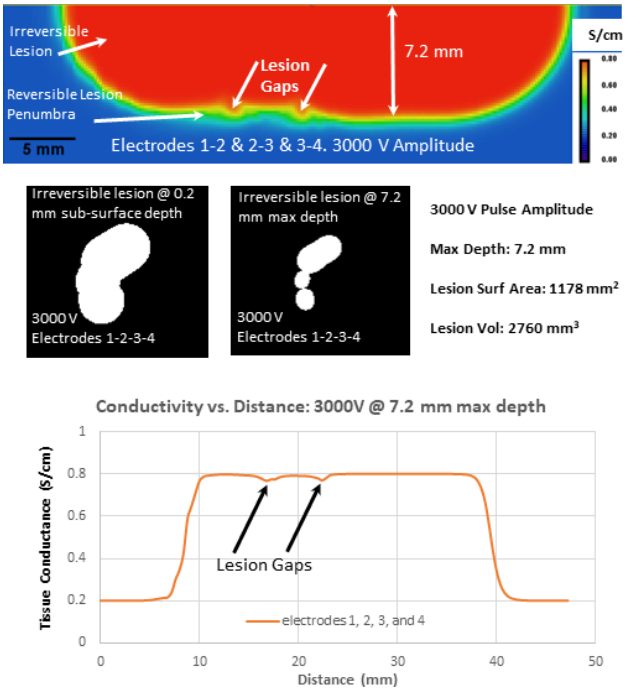

Figure 4. Model-predicted tissue conductance profile and lesion geometry (sub-surface and at max depth) achieved at 3000 V pulse amplitude. Note the onset of gaps at the max connected lesion depth of 7.2 mm.

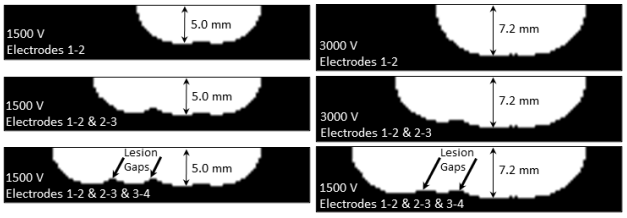

Figure 5. Transverse views through the model-predicted lesion profiles showing a comparison of the overall geometry of the lesions achieved using a 1500 V vs. 3000 V pulse amplitude across electrodes 1 & 2, 1, 2 & 3, and 1, 2, 3 & 4.

pulse trains, with the most significant impedance decrease following the first pulse and additional, less significant impedance decrease observed with each subsequent pulse [10]. These findings also corroborate our model-predicted tissue conductance increase (and hence impedance decrease) following irreversible elecroporation.

4. Conclusions and Future Work

The proposed quasi-dynamic model yields tissue conductance maps, predicts the fully irreversible lesion and reversible lesion penumbra at end electroporation, and confirms larger lesions with higher pulse amplitudes. Future work will focus on modeling time-based tissue response given specific pulse duration and delivery of sequential pulse trains, as well as the comparison of numerical and experimental results.

Acknowledgements

This work was supported by grants from the National Science Foundation (Award No. 1808530) and the National Institutes of Health (Award No. R35GM128877).

References

[1] Linte CA, Camp JJ, Holmes 3rd DR, Rettmann ME, Robb RA. Toward online modeling for lesion visualization and monitoring in cardiac ablation therapy. Lect Notes Comput Sci 2013;8149:9–17.

[2] Linte CA, Camp JJ, Rettmann ME, Haemmerich D, Aktas MK, Huang DT, Packer DL, Holmes 3rd DR. Lesion modeling, characterization, and visualization for image-guided cardiac ablation therapy monitoring. J Med Imaging 2018; 5:021218–01–15.

[3] Calkins H, Hindricks G, Cappato R*et al.* 2017 HRS/EHRA/ECAS/APHRS/SOLAECE expert consensus statement on catheter and surgical ablation of atrial fibrillation. Heart Rhythm 2017;14:e275–e444.

[4] Bradley CJ, Haines DE. Pulsed field ablation for pulmonary vein isolation in the treatment of atrial fibrillation. J Cardiovasc Electrophysiol 2020;31:2136–47.

[5] Muthalaly RG, John RM, Schaeffer B, Tanigawa S, Nakamura T, Kapur S, Zei PC, Epstein LM, Tedrow UB, Michaud GF, Stevenson WG, Koplan BA. Temporal trends in safety and complication rates of catheter ablation for atrial fibrillation. I Cardiovasc Electrophysiol 2018; 29:854–60.

[6] Weaver JC. Electroporation of cells and tissues. IEEE Trans Plasma Sci 2000;28:23–33.

[7] Mali B, Jarm T, Corovic S, Paulin-Kosir MS, Cemazar M, Sersa G, Miklavcic D. The effect of electroporation pulses on functioning of the heart. Med Biol Engi Comput 2008; 46:745–57.

[8] Prado LNS, Goulart JT, Zoccoler M, Oliveira PX. Ventricular myocyte injury by highintensity electric field: effect of pulse duration. Gen Physiol Biophys 2016;35:121–30.

[9] Corovic S, Lackovic I, Sustaric P, Sustar T, Rodic T, Miklavcic D. Modeling of electric field distribution in tissues during electroporation. BioMedcial Engineering Online 2013;12:1–27.

[10] Shah KB, Mehta NK, Kutinsky IB, Stewart MT, Verma A, Calkins H, Boersma LVA, Haines DE. Pulsed field ablation trains reduce tissue impedance in patients undergoing pulmonary vein isolation. Heart Rhythm 2021;18:S1–S546.

Address for correspondence:

Cristian A. Linte, PhD. Biomedical Engineering, Rochester Institute of Technology. 160 Lomb Memorial Dr. Rochester NY 14623 USA. Email: clinte@mail.rit.edu.